Method for Determining the Depth of the Shower Maximum Using Pulse Width Data from the TAIGA-HiSCORE Cherenkov Array

NUCLEUS – 2025. Nuclear physics and elementary particle physics. Nuclear physics technologies.

[1] Mark Ternovoy, TAIGA collaboration

[1]Research Institute of Applied Physics of Irkutsk State University.

The work was supported by the Russian Science Foundation, grant №23-72-00016 (section 2) and Irkutsk State University (project № 091-25-309).

Saint Petersburg, SPbU, July 4, 2025

Physics of Extensive Air Showers (EAS)

- Any cosmic particle colliding with an atmospheric particle generates a cascade of secondary particles — **an extensive air shower**.
- The interaction occurs with atmospheric molecules, primarily nitrogen and oxygen, at altitudes of 10–20 km.
- A primary particle with an energy of 10^{12}–10^{19} eV, upon colliding with an atomic nucleus, produces numerous secondary particles such as pi-mesons, electrons, positrons, muons, and gamma quanta.

- **The development of an EAS depends on the energy and type of the primary particle, as well as the density of the atmosphere.** The main characteristics of the shower, such as the number of particles, their energy, and spatial distribution, allow for the determination of the properties of the primary cosmic radiation.

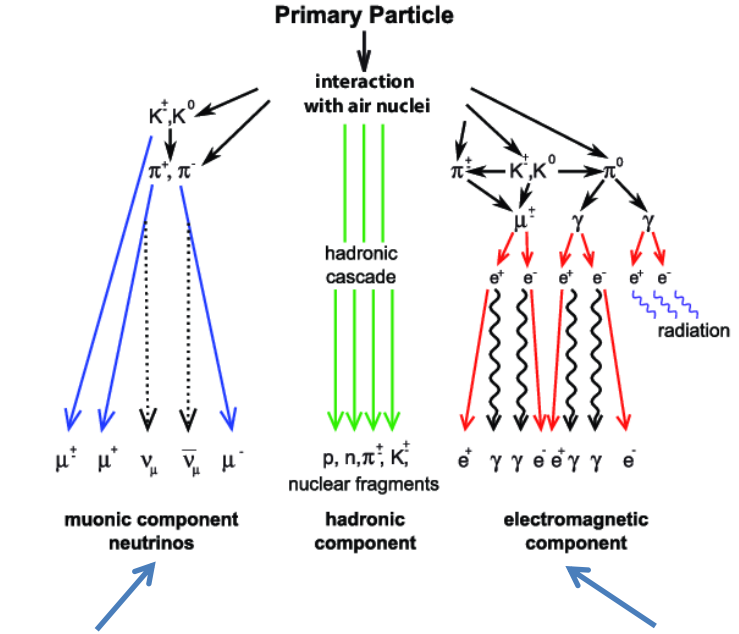

Provides information about the particle's mass

Provides information about the particle's energy

Physics of Extensive Air Showers (EAS)

- As the number of particles increases, the energy per particle decreases.

- The number of particles (or, with less uncertainty, the amount of energy transferred to secondary particles and ultimately released into the atmosphere) reaches **a maximum at a certain depth X_{max}, which is a function of energy, determines the nature of the primary particle.**

$$X_{max} \propto \ln \frac{E_0}{A}$$

- In EAS, Cherenkov light is emitted by relativistic particles, such as electrons and positrons, formed in the cascade. This light forms a cone with a small opening angle (about 1–2 degrees in the atmosphere), which is detected by ground-based detectors.

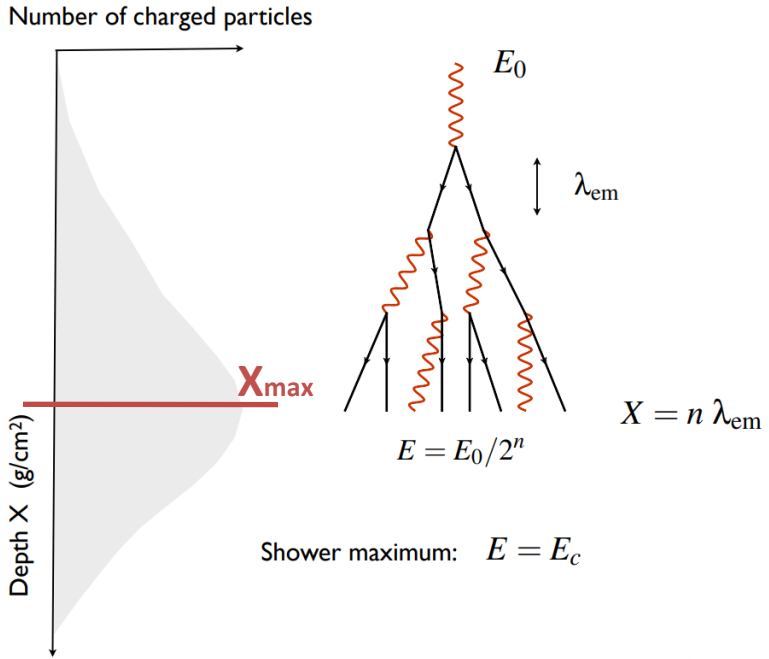

General Characteristics of the Cosmic Ray Energy Spectrum

- **Spectrum Shape:** The cosmic ray energy spectrum follows a power law $J(E) = E^{-\gamma}$, where J(E) is the particle flux, E is the primry energy, and **γ** is the spectral index.
- The value of **γ** varies across different energy ranges:
  - Up to ~3×10^{15} eV (**knee**): **γ**≈2.7.
  - Between $3\times10^{\wedge15}$ and ~4×10^{17} eV: < **γ**≈3.0–3.1 (**second knee**).
  - Above the ~4×10^{18} eV (**ankle**): **γ**≈2.6–2.7.

- **Energy Range:** The spectrum spans over 11 orders of magnitude, from low-energy particles (galactic sources) to ultra-high-energy particles (extragalactic sources).

- **Measurements:** The spectrum is measured using direct methods (detectors on satellites and balloons, up to ~10^{14} eV) and indirect methods (EAS detection, above 10^{14} eV).

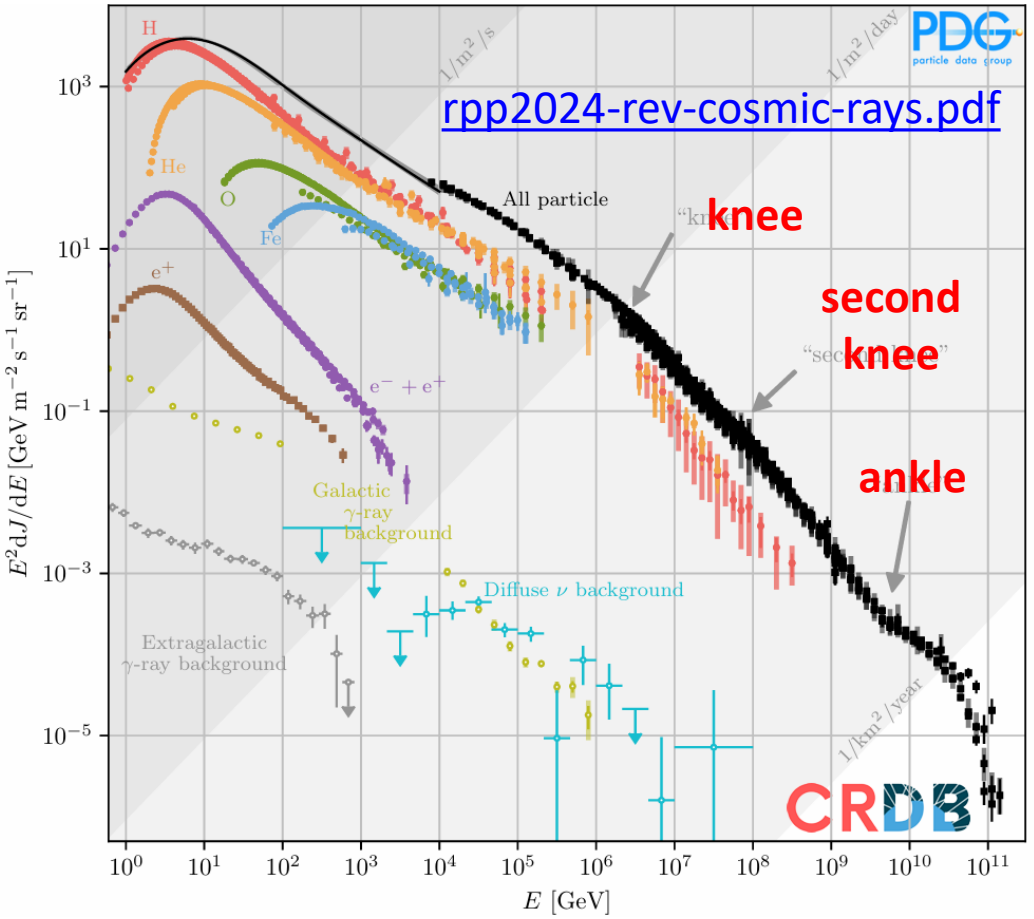

General Characteristics of the Cosmic Ray Energy Spectrum

- **Mass Composition:**
  - **Light nuclei (protons, helium):** Dominate at low energies (<10^{15} eV). Their fraction decreases around **the knee** due to faster energy loss in magnetic fields.
  - **Heavy nuclei (carbon, oxygen, iron):** Become significant around the knee and second knee. Their greater rigidity ($E_{max} \propto Z$) allows them to reach higher energies in galactic accelerators. Controversial Claims:
- **Controversial Claims:**
  - The fraction of light particles decreases above the knee but may increase around the ankle (confirmed by Pierre Auger, disputed by Telescope Array).
  - Carbon, oxygen, and iron dominate in the 10^{15}–10^{18} eV range.

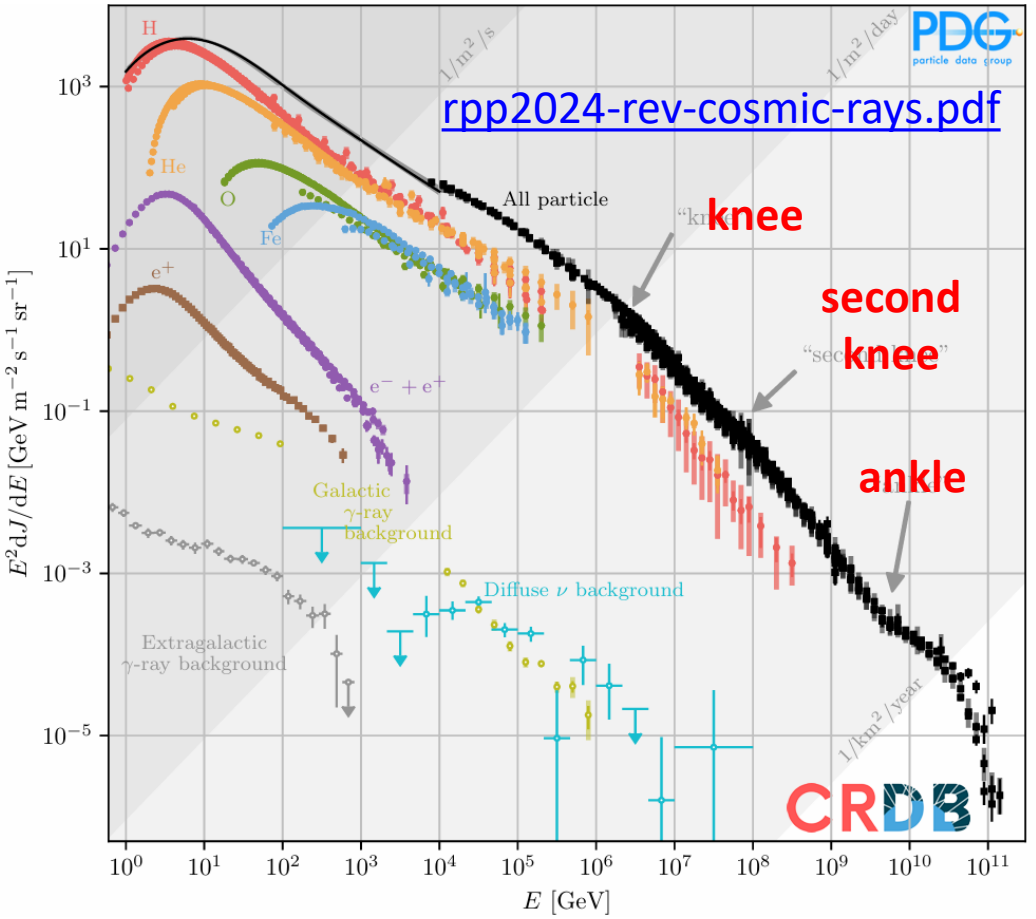

General Characteristics of the Cosmic Ray Energy Spectrum

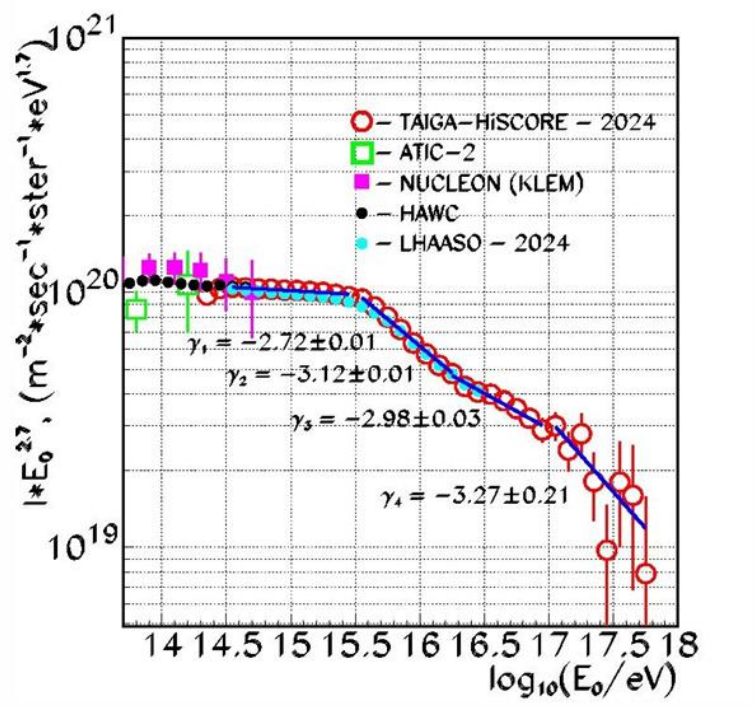

Differential energy spectrum of cosmic rays based on data from the TAIGA-HiSCORE array for stations oriented at the zenith (7,950,000 events).

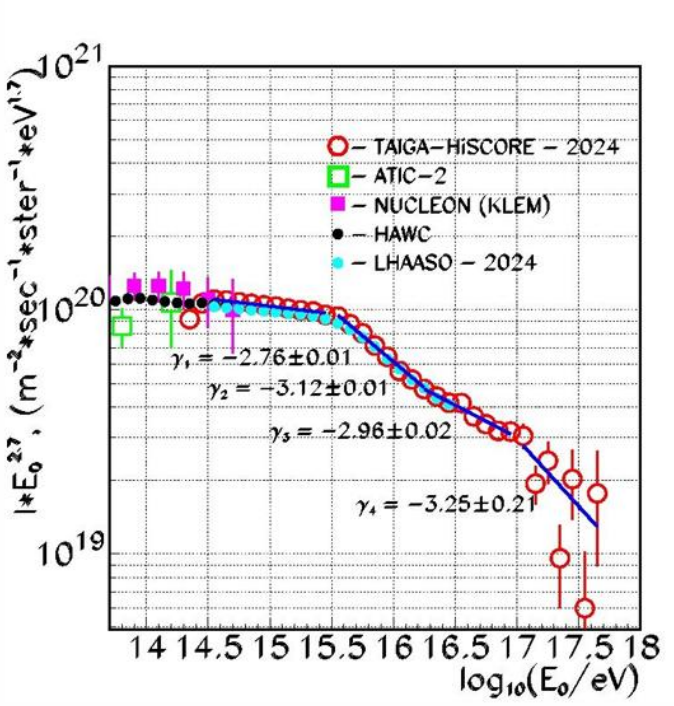

Differential energy spectrum of cosmic rays based on data from the TAIGA-HiSCORE array for stations oriented southward at a 25° zenith angle (10,600,000 events).

TAIGA-1 Gamma Observatory

- 2010 and Present: Tunka Advanced Instrument for cosmic rays and Gamma Astronomy; Tunka Valley, Buryatia, Russia (50 km from Lake Baikal)

Tunka-133

TAIGA-HiSCORE

TAIGA-IACT

Tunka-Grande

TAIGA-Muon

TAIGA-1

- Includes:
  - **TAIGA-HiSCORE: 114 Cherenkov stations over an area of 1.1 km², gamma-ray threshold ~50 TeV.**
  - **TAIGA-IACT:** 3 telescopes (2017, 2019, 2022), threshold 2–3 TeV, field of view 9.6°.
  - **Tunka-Grande:** 19 scintillation stations for energies >1 PeV.
  - **TAIGA-Muon:** Prototype muon detectors (several clusters, currently on hold).
- Achievements of TAIGA:
  - Observation of the Crab Nebula with a significance of 12σ over 150 hours.
  - Study of the light component of cosmic rays (protons and helium) with confirmation of a spectral break at ~3 PeV.
  - Cosmic ray energy spectrum with varying slopes in the 1–100 PeV range.
  - Successful detection of gamma-ray bursts based on GCN alerts.

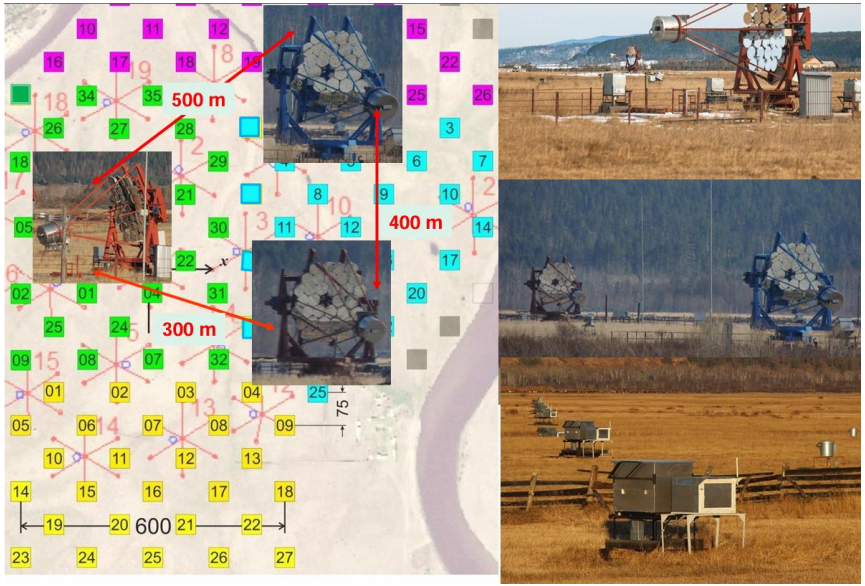

Current Status of the TAIGA-HiSCORE Array

- The array covers an area of up to 1 km² with 114 stations in **zenith** (2022-2023 season, autumn 2023) or **inclined** orientation (2021-2022, 2023-2025);
- In full configuration with 4 clusters – **from 2021 to the present.**
- Each station is equipped with a set of four large photomultiplier tubes (PMTs). **The time resolution of each station is 10 ns. Time step is 0.5 ns.**

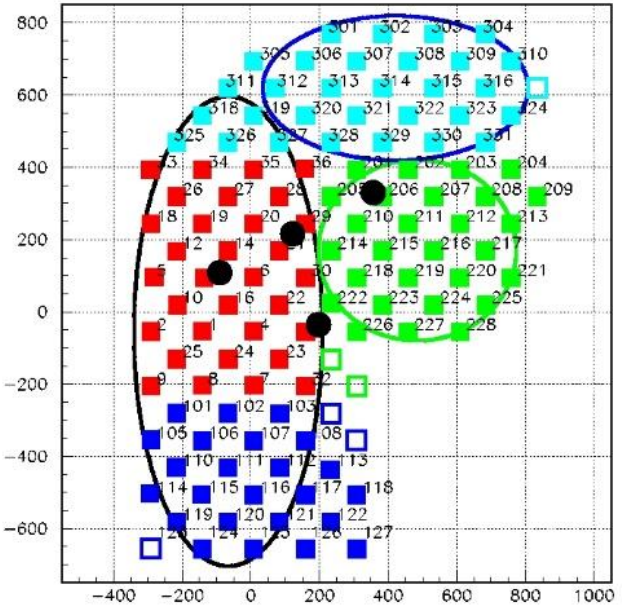

Methods for Measuring EAS Maximum Depth

- **10^{18} - 10^{20} eV**

  Direct observation of X_{max} through ionization light, as in the Pierre Auger and Telescope Array experiments.

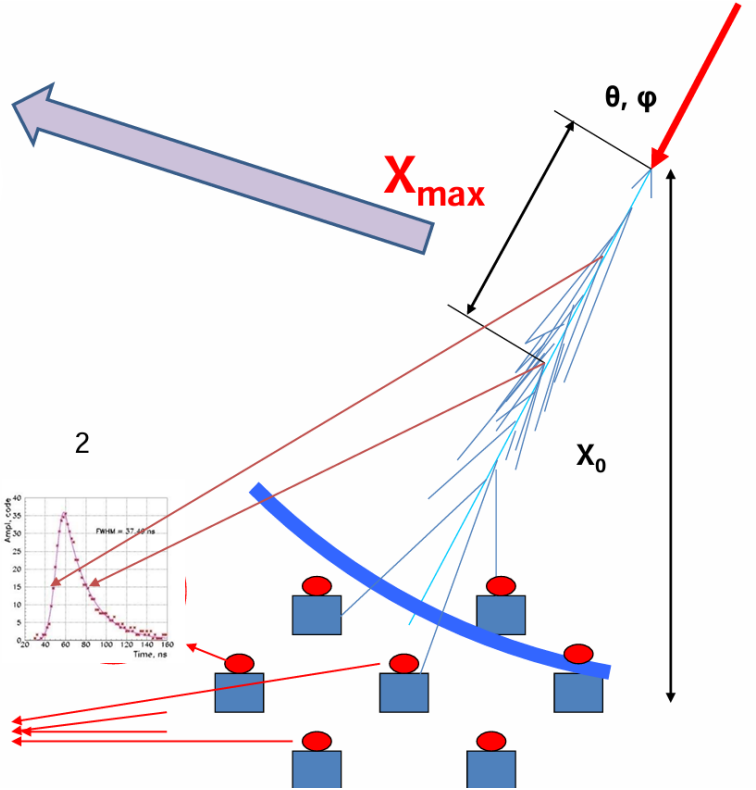

- **10^{15} - 10^{18} eV**

Two methods for estimating X_{max}:

- Steepness of the spatial light distribution function (LDF): **P** = $Q(R_1)/Q(R_2)$, $R_2 > R_1$ **(P-method).**
- Pulse width at half-height (FWHM), **$\tau_{1/2}$ (τ-method).**

Similarity of Cascade Curves

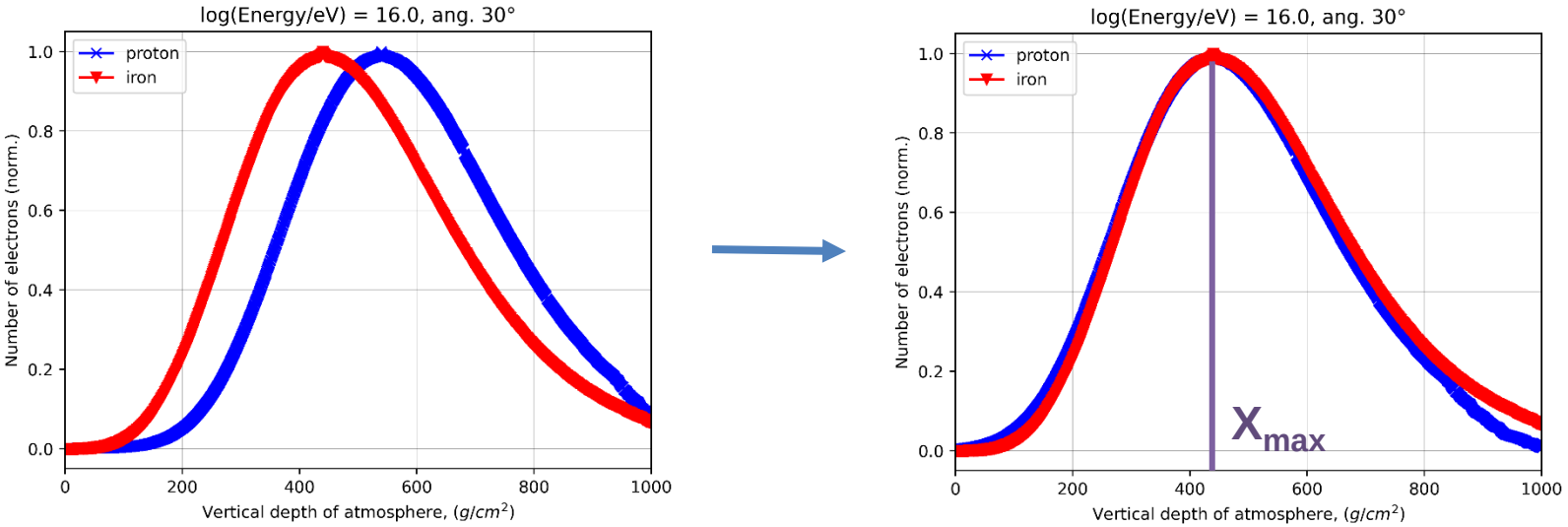

- Cascade curves describe the electron density in a shower as a function of atmospheric depth;
- The shapes of cascade curves, which determine the electron density in a shower as a function of atmospheric depth, are nearly identical for different types of primary particles. CORSIKA simulations confirm this fact;
- **Therefore, the shower maximum depth X_{max} can be considered the primary parameter for assessing the mass composition**.

X_{max} Dependence on Primary Composition

- **The difference between primary compositions at 10 PeV (lg (E/TeV) = 4) can be divided into approximately 4 equal parts:**
  - Proton – 630 g/cm²;
  - Helium – 590 g/cm²;
  - Nitrogen – 550 g/cm²;
  - Iron – 510 g/cm².

The difference between proton and iron compositions is ~120 g/cm²;

Proton

$$X_{max} = -1.798 \cdot \log E/TeV^2 - 71.355 \cdot \log E/TeV + 373.53$$

Iron

$$X_{max} = -3.888 \cdot \log E/TeV^2 - 103.00 \cdot \log E/TeV + 160.76$$

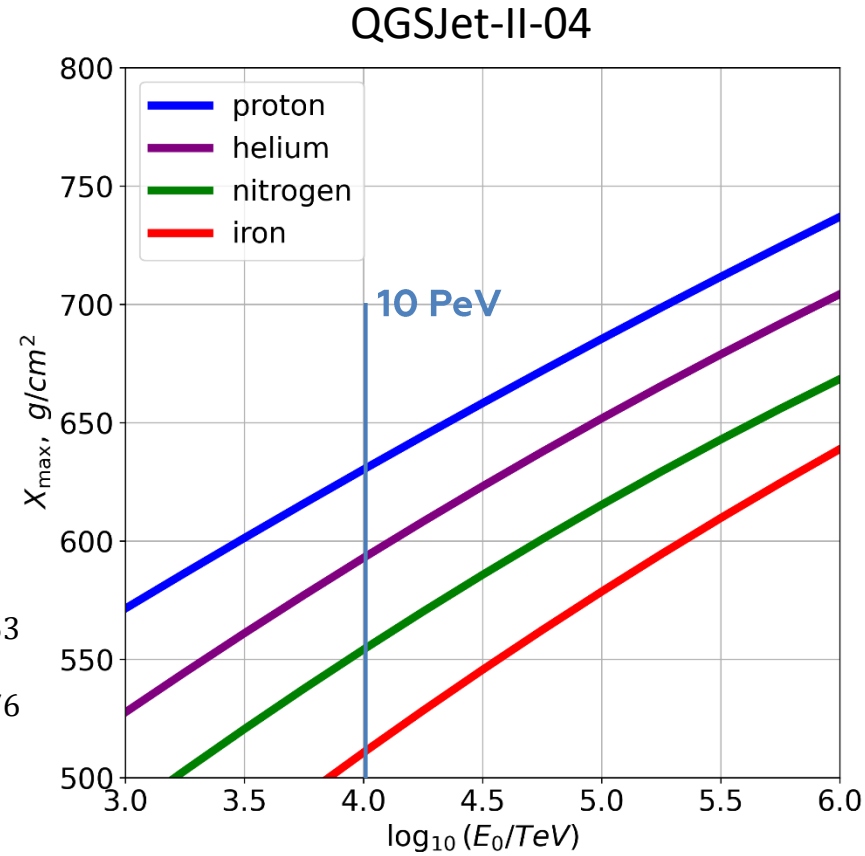

Simulations for X_{max} Determination Methods

- To analyze the possibility of determining the shower maximum depth using methods applied at HiSCORE, simulations were conducted with the following parameters:
  - **CORSIKA**+(**QGSJet-II-04** or **Sybill2.3d**) + **GHEISHA2002d**;
  - Primary energy: 1,3,10,30,100 PeV;
  - Angles: 0, 30°;
  - Primary particles: proton, helium, iron;
  - No statistical thinning;
  - **The Cherenkov light simulation option was also used (bunch=1 ph), which significantly increased the computational time per shower (by 15-20 times).**

Pulse Width (FWHM) Measurement at HiSCORE

- To estimate pulse duration in the experiment, signals from the anode channels of PMTs are used. The general data processing algorithm includes several stages:
    - Signals are time-shifted by 0.5 nanoseconds to improve measurement accuracy;
    - Signals from four PMTs at a single station are summed to obtain the resulting pulse;
    - After summation, the resulting pulses are convolved with the station's instrumental function.

  The instrumental function is characterized by a duration of about 10 nanoseconds for anode channels.
    - To account for instrumental effects, pulses from simulations (CORSIKA) are convolved with these characteristics to reproduce their behavior in the real experiment.

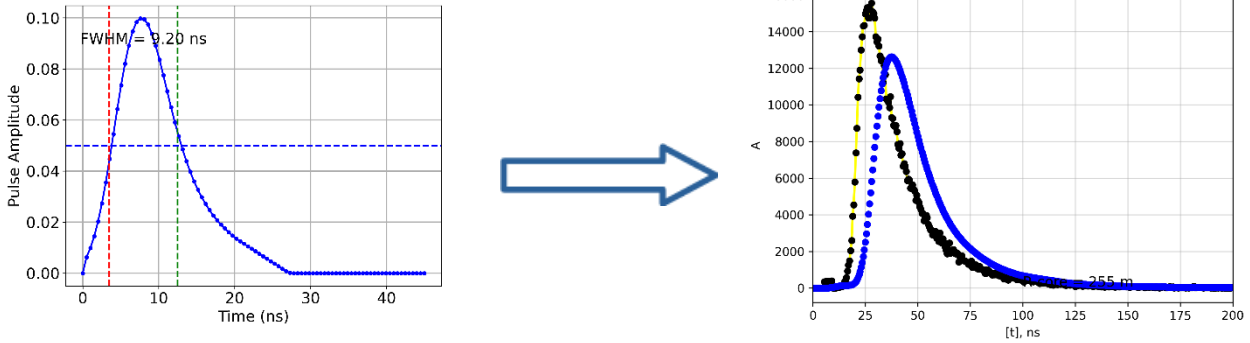

τ-Method for Determining X_{max}

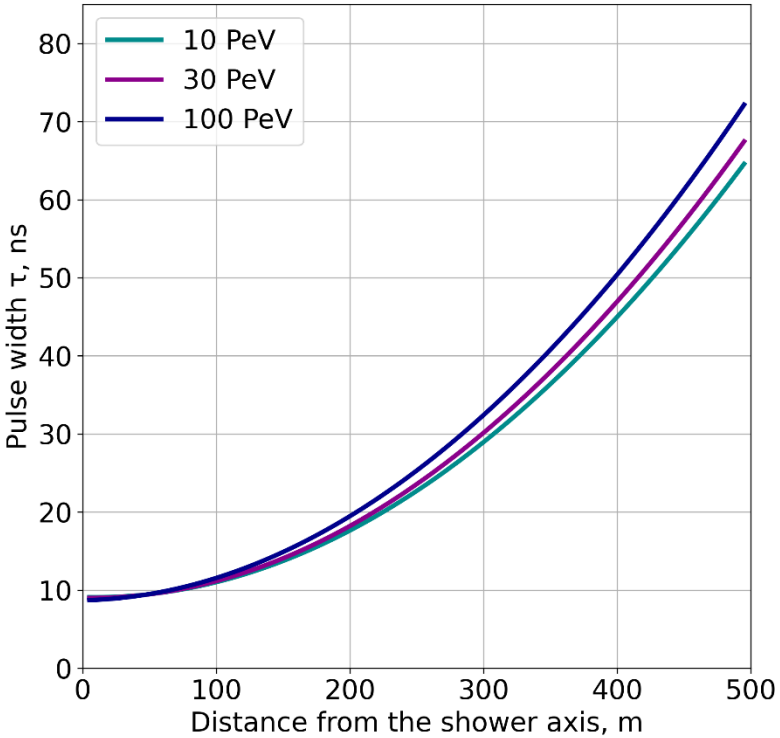

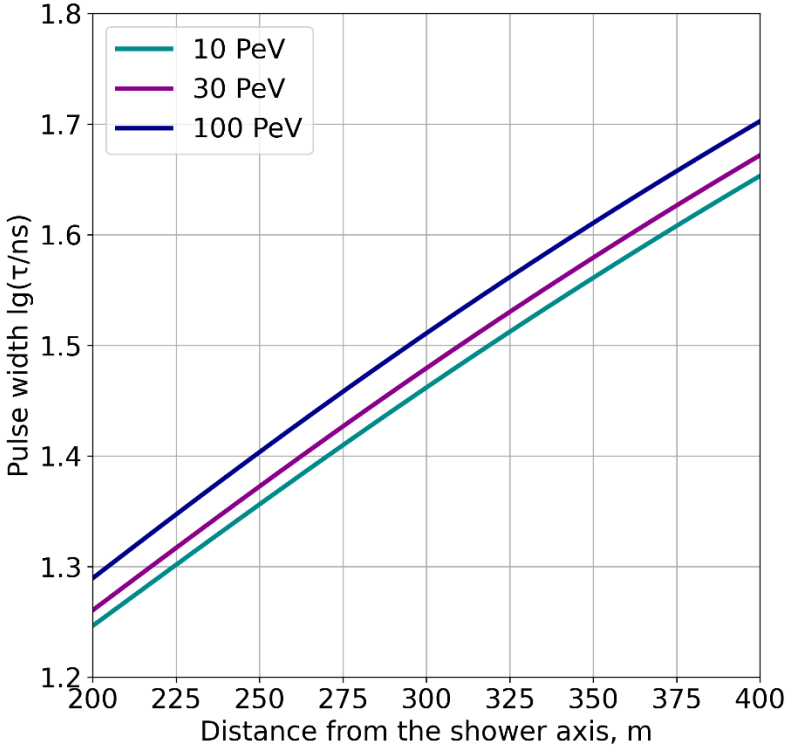

- **According to simulation data, pulse duration increases with distance.**

τ-Method for Determining X_{max}

- **Point distributions are compiled from primary compositions for energies of 10, 30, 100 PeV and two angles (0-30°), with an instrumental function of FWHM = 9.2 ns.**

- **Anode Channel:**
  - 205 м: $\Delta X_{max} = -1465.0 \cdot \log\tau + 2291.1$,
  - 255 м: $\Delta X_{max} = -1333.2 \cdot \log\tau + 2274.8$, $\sigma = \pm 10.17\ \mathrm{g/cm^2}$
  - **305 м: $\boldsymbol{\Delta X_{max} = -1244.3 \cdot \log\tau + 2285.5}$, $\boldsymbol{\sigma = \pm 11.30\ \mathrm{g/cm^2}}$**
  - 355 м: $\Delta X_{max} = -1212.3 \cdot \log\tau + 2360.9$,
  - 405 м: $\Delta X_{max} = -1205.7 \cdot \log\tau + 2462.0$,

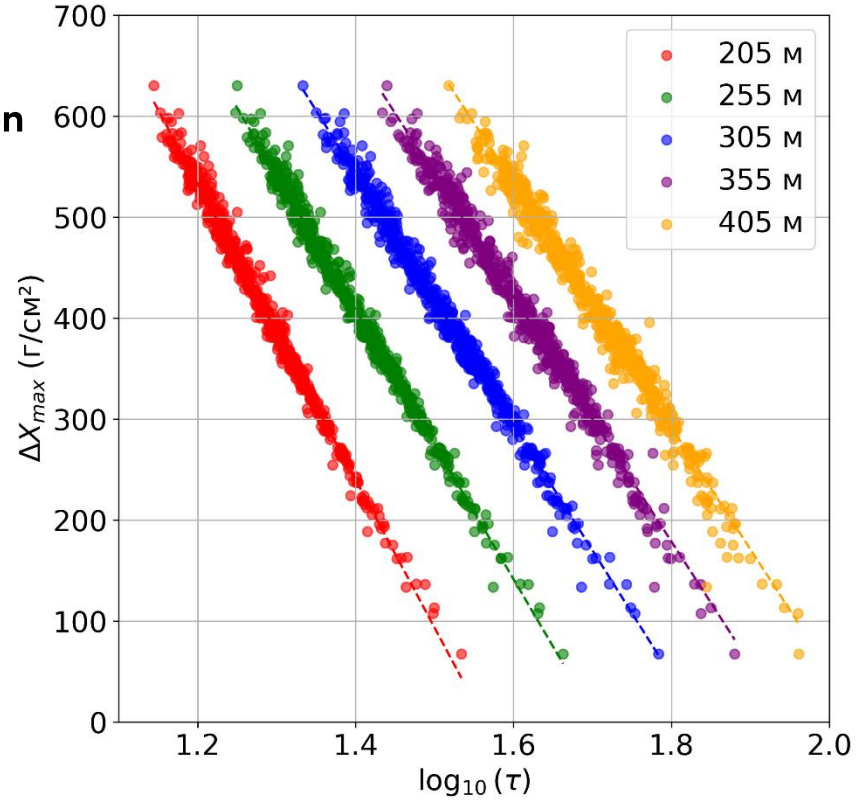

Correlation of X_{max} Relative Position and LDF Steepness

- Steepness: $P = Q(80)/Q(200)$ (parameter introduced in 2021);
- Relative position of the maximum: $\Delta X_{max} = X_0/\cos\theta - X_{max}$ (relative to the observation array);
- The shower maximum depth is determined using the ratio of light flux at distances of 80 and 200 m from the axis.

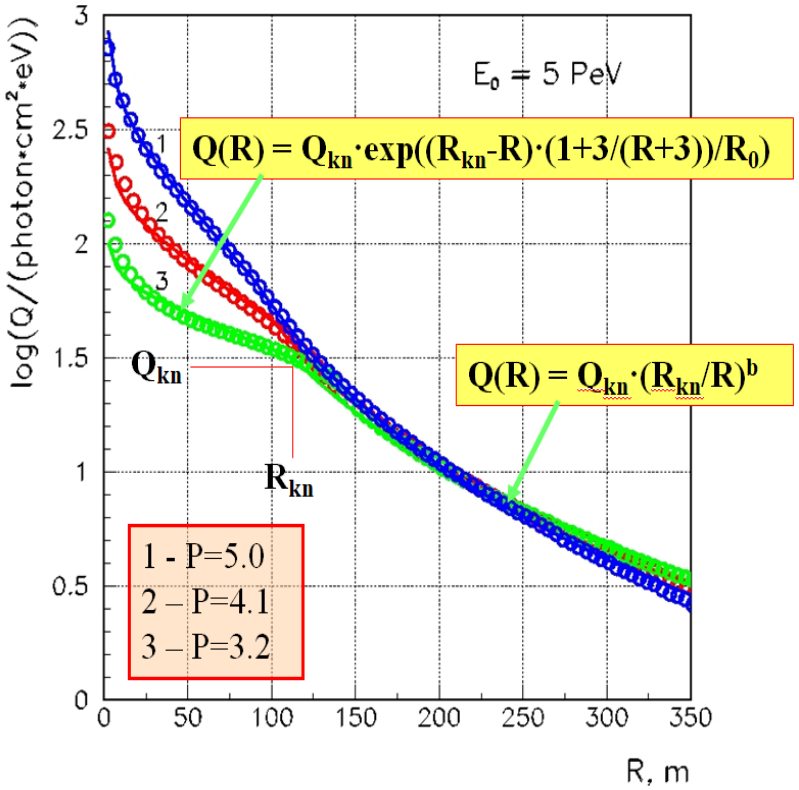

P vs ΔX_{max} Dependence

- Good fit, only p+He, 0-30°:
  $\Delta X_{max} = -98 \cdot P + 922$, σ= ±17.28 g/cm²

- The experimental steepness distribution is within the sensitivity of P to ΔX_{max} under the given constraints on zenith angle and energy.
- The transformation from parameter P to ΔX_{max} is independent of:
  - Energy (10^{15} – 10^{16} eV),
  - Zenith angle of the shower (0° - 30°),
  - Hadron interaction model.

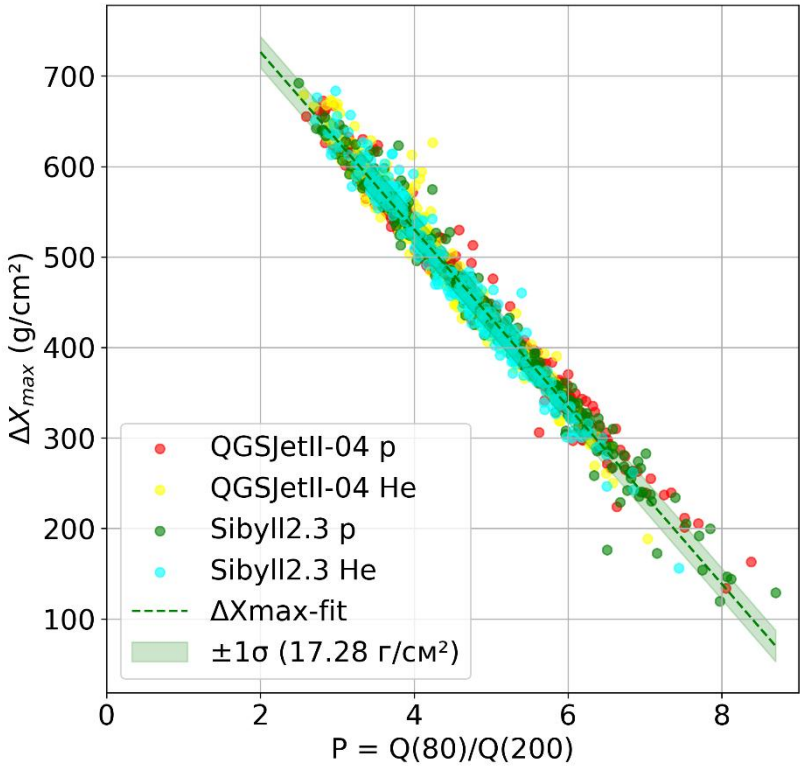

Experimental Dependence of $\langle X_{max} \rangle$ on Primary Energy

- **TAIGA-HiSCORE:**
  - For the **τ-method**: vertical configuration of the 2022-2023 season, 3383 events in the 10-130 PeV range;
  - 29 events above 100 PeV, 844 events at >30 PeV.

  - For the **P-method**: 2021-2024 seasons, 905283 events <30 PeV.

  - 4 clusters (114 stations);
  - Zenith angles θ ≤ 30°;
  - Effective area 1 km².

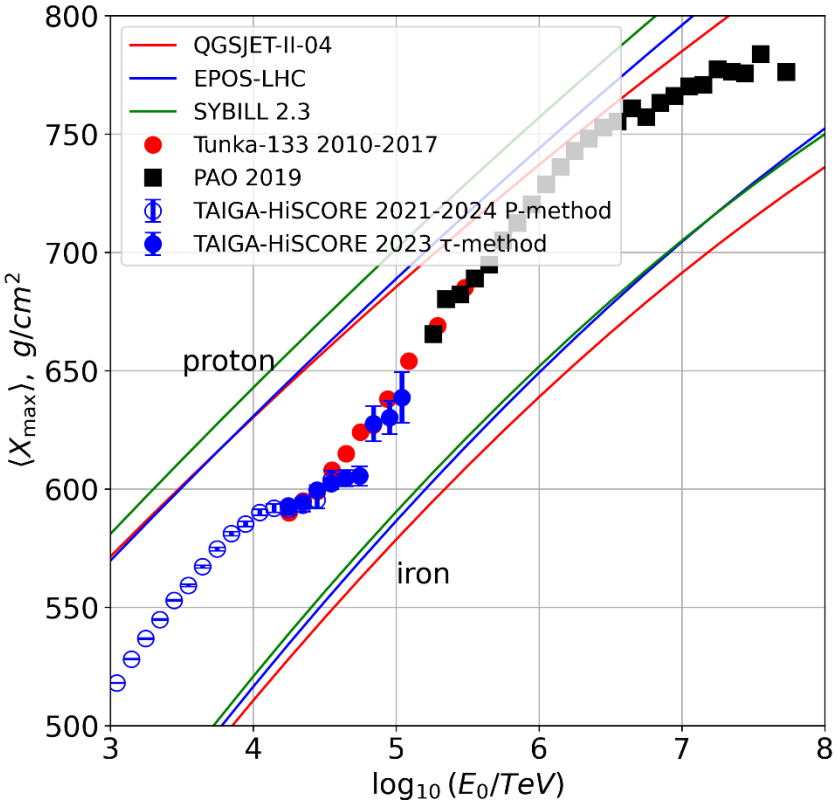

Average Mass Composition $\langle \ln A \rangle$

- Direct dependence $\langle \ln A \rangle \sim \langle X_{max} \rangle$ by linear interpolation:

$$\langle \ln A \rangle = \frac{X_{max}^{p} - X_{max}^{data}}{X_{max}^{p} - X_{max}^{Fe}} \cdot \ln 56$$

- The **QGSJet-II-04** model was used to recalculate $\langle \ln A \rangle$.

- For comparison, data from the LHAASO, Pierre Auger Observatory, Telescope Array, TALE and Tunka-133 experiments were used.

- Across the entire energy range, a slightly lighter composition (p + He) is observed, but there is a range where the composition becomes heavier.

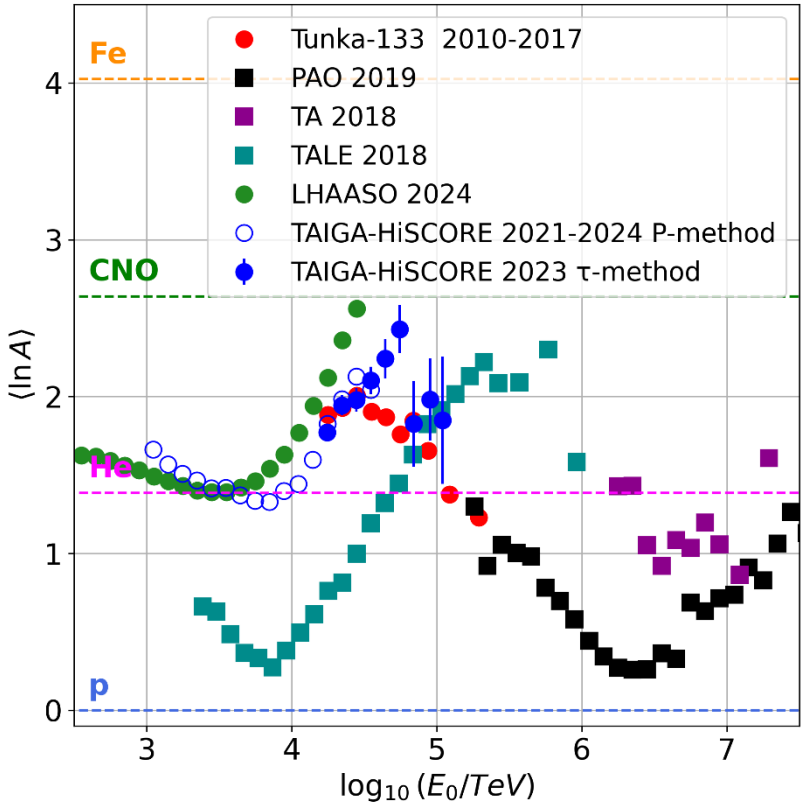

Conclusion

- Two independent methods for reconstructing the EAS maximum depth (X_{max}) based on TAIGA-HiSCORE data have been developed:
  - The **P-method**, using the steepness parameter of the Cherenkov light spatial distribution function ($P = Q(80)/Q(200)$),
  - The **τ-method**, based on the pulse width at a distance of 305 m from the shower axis.

- Linear dependencies for converting parameters P and τ_{305} to ΔX_{max} were established through CORSIKA shower simulations, with a reconstruction accuracy of 10–17 g/cm².
  - For the τ-method, the experimental statistics will increase by 3 times; new improvement - take into account noises for pulses in simulations."

- Based on TAIGA-HiSCORE data from the 2021–2024 seasons, the average maximum depth $\langle X_{max} \rangle$ and the average logarithm of the atomic number $\langle \ln A \rangle$ were determined, confirming the heavier composition of cosmic rays in the $3 \cdot 10^{15} - 3 \cdot 10^{16}$ eV range and its lighter composition at energies above $3 \cdot 10^{16}$ eV.